

# Estimation of source apportionment and potential source locations of PM<sub>2.5</sub> at a west coastal IMPROVE site

InJo Hwang, Philip K. Hopke\*

*Department of Chemical and Biomolecular Engineering and Center for Air Resources Engineering and Science,  
Clarkson University, Box 5708, Potsdam, NY 13699-5708, USA*

Received 29 April 2006; accepted 18 August 2006

---

## Abstract

Particle composition data for PM<sub>2.5</sub> samples collected at Kalmiopsis Interagency Monitoring of Protected Visual Environments (IMPROVE) site in southwestern Oregon from March 2000 to May 2004 were analyzed to provide source identification and apportionment. A total of 493 samples were collected and 32 species were analyzed by particle induced X-ray emission, proton elastic scattering analysis, photon-induced X-ray fluorescence, ion chromatography, and thermal optical reflectance methods. Positive matrix factorization (PMF) was used to estimate the source profiles and their mass contributions. The PMF modeling identified nine sources. In the Kalmiopsis site, the average mass was apportioned to wood/field burning (38.4%), secondary sulfate (26.9%), airborne soil including Asian dust (8.6 %), secondary nitrate (7.6%), fresh sea salt (5.8%), OP-rich sulfate (4.9%), aged sea salt (4.5 %), gasoline vehicle (1.9%), and diesel emission (1.4%). The potential source contribution function (PSCF) was then used to help identify likely locations of the regional sources of pollution. The PSCF map for wood/field burning indicates there is a major potential source area in the Siskiyou County and eastern Oregon. The potential source locations for secondary sulfate are found in western Washington, northwestern Oregon, and the near shore Pacific Ocean where there are extensive shipping lanes. It was not possible to extract a profile directly attributable to ship emissions, but indications of their influence are seen in the secondary sulfate and aged sea salt compositions.

© 2006 Elsevier Ltd. All rights reserved.

**Keywords:** PM<sub>2.5</sub>; IMPROVE; Source profile; Mass contribution; PMF modeling; PSCF analysis

---

## 1. Introduction

In order to protect visibility in the mandatory Class 1 areas (national parks and wilderness areas) from anthropogenic air pollutants, the inter-agency monitoring of protected visual Environments (IMPROVE) monitoring program was established in

1985. The goals of the IMPROVE program are (1) to provide visibility and aerosol data in mandatory Class 1 areas, (2) to measure the chemical compositions of air pollutants that lead to visibility degradation, (3) to establish long-term data to support national visibility improvement goals (Malm et al., 1994; <http://vista.cira.colostate.edu/improve/>). The IMPROVE program gives priority to visibility-related research, including the advancement of monitoring instruments, analysis techniques of chemical compositions, visibility modeling, strategies to manage air quality, and

---

\*Corresponding author. Tel.: +1 315 268 3861;  
fax: +1 315 268 4410.

E-mail address: [hopkepk@clarkson.edu](mailto:hopkepk@clarkson.edu) (P.K. Hopke).

source attribution studies (Zhao and Hopke, 2004, 2006; Kim and Hopke, 2006).

Since  $\text{PM}_{2.5}$  is adverse to human health and welfare and causes visibility degradation (Schwartz et al., 1996; Chan et al., 1999; Harrison and Yin, 2000; Calcabrini et al., 2004), many countries are developing and implementing environmental policies to control  $\text{PM}_{2.5}$  by establishing ambient air quality standards for  $\text{PM}_{2.5}$  and evaluating the sources of the ambient  $\text{PM}_{2.5}$ . The US Environmental Protection Agency (EPA) promulgated the new regulations that established National Ambient Air Quality Standards (NAAQS) for  $\text{PM}_{2.5}$  in 1997 (US Environmental Protection Agency, 1998). As part of the management of ambient air quality, it is necessary to identify sources and to apportion the ambient PM mass. Sources of  $\text{PM}_{2.5}$  are also sources of visibility degradation and therefore source apportionment studies derived for  $\text{PM}_{2.5}$  are also used for understanding visibility problem. To do so, receptor models have been developed that analyze various properties of the pollutants at the receptor site and estimate the source contributions (Hwang and Hopke, 2006).

The objective of this project is to resolve the sources of  $\text{PM}_{2.5}$  with a particular emphasis on the impacts of ship emissions on the mass concentrations observed along the west coast of the United States. Ship engines burn low cost residual oil similar to that used in oil-fired power plants.

Corbett and Fishbeck (2000) have estimated the impacts of ship emissions on  $\text{NO}_x$  and  $\text{SO}_2$  and suggest that there could be an influence along the west coast from Seattle to San Diego. The ability of these analyses to separately apportion the impacts of ships, spark- and compression-ignition vehicle emissions, as well as the formation of secondary carbon will be important to permit the assessment of the effects of ship emissions on air quality along the coasts. Positive matrix factorization (PMF) was applied to identify the existing sources and apportion the  $\text{PM}_{2.5}$  mass to each source. In addition, after the source profiles and source apportionments were resolved, potential source contribution function (PSCF) was applied to identify the potential source locations by combining with each source apportionment values.

## 2. Experimental methods

### 2.1. Sample collection and analytical methods

$\text{PM}_{2.5}$  samples were collected at Kalmiopsis IMPROVE site (latitude 42.552, longitude  $-124.0589$ , 80 m above sea level)(Fig. 1). This site is a wilderness area, and located near the Klamath Mountains of southwestern Oregon. There are no large local roads or highways. This site is located about 56 km east of Interstate Highway 5 and about 30 km east of the Pacific Ocean and US Highway

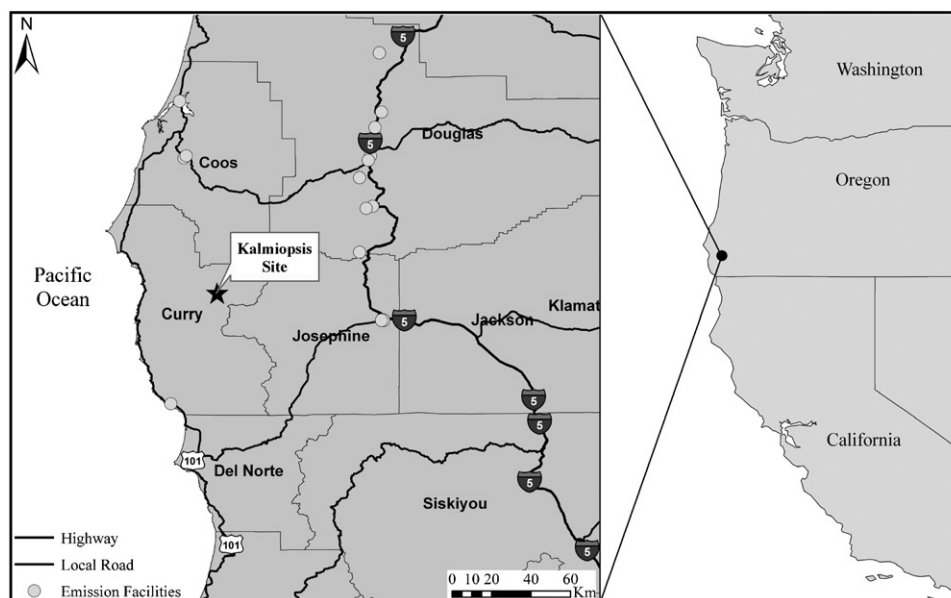


Fig. 1. Location of the Kalmiopsis IMPROVE site and major facilities emitted  $\text{PM}_{2.5}$  sources.

101. The nearest city is Grants Pass, Oregon about 60 km to the east of the sampling site, with a population about 25,000. There are approximately 15 PM<sub>2.5</sub> emitting facilities in the area according to the emission inventory (US Environmental Protection Agency, 2005). The primary industry in the area is timber production.

The PM<sub>2.5</sub> samples were collected using the IMPROVE sampler (Huffman, 1996). Teflon, nylon, and quartz filters were used to collect PM<sub>2.5</sub> samples. The detailed filter analyses methods are reported in previous studies (Malm et al., 1994; Liu et al., 2003a, b). The quartz filters were used for organic carbon (OC) and elemental carbon (EC) by thermal optical reflectance (TOR) method (Chow et al., 1993). Total carbon is separated into eight carbon fractions, defined by temperature and oxidation atmosphere (Chow et al., 2001, 2005; Kim and Hopke, 2005). A total of 493 samples were obtained from March 2000 to May 2004 for the Kalmiopsis IMPROVE site.

## 2.2. PMF modeling

PMF (Paatero, 1997) was applied to the data as implemented using the PMF2 program. PMF2 has been used in a number of prior studies (e.g., Ramadan et al., 2000; Polissar et al., 2001a, b; Lee et al., 2002; Kim et al., 2003; Kim and Hopke, 2004a, b; Begum et al., 2005; Hwang and Hopke, 2006). The application of PMF depends on the error estimate for each of the measured data (Polissar et al., 1998). Each data point is assigned an uncertainty that is used in this weighted least squares regression. Increasing the error estimates permits the reduction in the influence of noisy data such as below detection limit (BDL) and missing values. Polissar et al. (1998) have suggested an approach for estimating the concentration values and their associated error estimates including BDL values and missing data, and this approach was used in this study. The data were screened using the signal to noise ratio (S/N ratio) criteria described by Paatero and Hopke (2003). Variables with very low S/N values (bad variables, S/N ratio  $\leq 0.2$ ) were excluded from the analysis while the weak variables ( $0.2 < \text{S/N ratio} < 2$ ) were downweighted.

In order to explore the rotational freedom, PMF used a parameter, FPEAK that controls addition and subtraction of the factors (Paatero et al., 2002). It is also possible to use pair-wise scatter plots of the *g*-vectors to help define the appropriate

FPEAK value (Paatero et al., 2005). In this study, FPEAK values between  $-1.0$  and  $1.0$  were examined. For these data, the value of FPEAK was chosen to be  $0.0$ .

## 2.3. Potential source contribution function

The PSCF is the conditional probability that an parcel with a certain level of pollutant concentrations arrives at a receptor site after having passed through a specific upwind source area (Ashbaugh et al., 1985; Gao et al., 1994; Hsu et al., 2003). In order to identify the potential locations of the regional sources of pollution, PSCF has been used in a number of prior studies (Polissar et al., 1999; Liu et al., 2003a, b; Zhou et al., 2004). The PSCF values were calculated using the source contributions and backward trajectories produced by the hybrid single particle Lagrangian integrated trajectory (HYSPLIT) model (Draxler and Rolph, 2003). PSCF<sub>*ij*</sub> is defined as

$$\text{PSCF}_{ij} = \frac{m_{ij}}{n_{ij}},$$

where  $n_{ij}$  is the total number of end points that fall in the *ij*th cell and  $m_{ij}$  is the number of end points in the same cell that are associated with samples that exceeded the threshold criterion. In this study, the average contribution of each source was used for the threshold criterion. If a trajectory is connected to a sample which has contribution higher than a selected criterion, all sequence end points of this trajectory are considered to be high. Therefore, a high PSCF value in a cell indicates a potential source area. Cells containing sources would be identified with conditional probabilities approaching 1 if trajectories that have crossed the cells effectively transport the emitted pollutant to the receptor site (Liu et al., 2003a, b).

In this study, in order to identify the potential locations of the regional sources of pollution, PSCF was calculated using the mass contribution of each source and backward trajectories data. Three-day backward trajectories were calculated every 6 h four times a day at 08, 14, 20, and 02 UTC (coordinated universal time) at height of 500 m above the ground level using the National Centers for Environmental Prediction/National Center for Atmospheric Research (NCEP/NCAR) re-analysis meteorological data. The total number of the end point was 143,664 and the geophysical region covered by the trajectories was divided into 74,880 grid cells of  $0.5^\circ \times 0.5^\circ$  latitude and longitude. Therefore, there are an average of 1.92

trajectory end points per cell. In order to reduce the effect of small values of  $n_{ij}$  that result in high PSCF values with high uncertainties, an arbitrary weight function  $W(n_{ij})$  was multiplied into the PSCF value to better reflect the uncertainty in the values for these cells (Polissar et al., 2001a). The PSCF values were down weighted when the total number of the end points per specific cell was less than about two times the average value of the end points per each cell.

$$W(n_{ij}) = \begin{cases} 1.00 & 4 \leq n_{ij}, \\ 0.75 & 2 < n_{ij} \leq 4, \\ 0.50 & 1 < n_{ij} \leq 2, \\ 0.15 & 0 < n_{ij} \leq 1. \end{cases}$$

### 3. Results and discussion

#### 3.1. Data analysis

For the Kalmiopsis site, 32 species (OC1, OC2, OC3, OC4, OP, EC1, EC2, EC3,  $\text{SO}_4^{2-}$ ,  $\text{NO}_3^-$ , Al, As, Br, Ca, Cl, Cr, Cu, Fe, H, K, Mg, Mn, Na, Ni, Pb, Rb, Se, Si, Sr, Ti, V, and Zn) were selected for PMF modeling and the weak variables (OC1, EC3, Cr, Mg, and V) were down weighted. IMPROVE data reported uncertainty and method detection limit (MDL) of each sample and each species. Any missing values or BDL values were replaced by the geometric mean of the concentration or average detection limit, respectively. Table 1 shows arithmetic mean, standard deviation, geometric mean, minimum value, maximum value, number of BDL, and S/N ratio for individual species during the sampling periods at sampling site.

#### 3.2. Source apportionment

In order to estimate the optimal number of sources, it is necessary to test different numbers of sources and estimate the optimal value with the most physically reasonable results. The scaled residual matrix,  $Q$  value, and the rotmat (rotational uncertainty) matrix were used to determine the number of sources. The rotmat matrix is a  $p \times p$  matrix of standard deviations of rotational coefficients, where  $p$  is the number of sources. The optimal number of sources was determined to be 9 based on examination of the scaled residuals and the  $Q$  value. Examination of the  $Q$  value as a function

of FPEAK was performed. To estimate source apportionment without multiple linear regression, the measured  $\text{PM}_{2.5}$  mass concentration was included as an independent variable in the PMF modeling (Kim and Hopke, 2006).

If specific species in the source profiles do not seem to be realistic based on comparisons with measured source profiles and prior analysis of similar data, it is possible to pull values toward zero to obtain the reasonable source profile used the FKEY matrix (Lee et al., 1999). This matrix of integer values has the same dimension as  $F$  matrix, where  $F$  matrix is a  $p \times m$  source profile matrix ( $m$  is the number of species). The details are reported in previous studies (Qin and Oduyemi, 2003; Zhao and Hopke, 2004). In this study, values of all elements were set to zero in the FKEY matrix, except for a value of six for Na in OP-rich secondary sulfate and aged sea salt, a value of six for  $\text{SO}_4^{2-}$  in nitrate, and a value of four for  $\text{SO}_4^{2-}$  in gasoline vehicle emissions. Fig. 2 shows the source profiles (value  $\pm$  standard deviation) obtained for the nine-factor PMF solution at the Kalmiopsis IMPROVE site. Fig. 3 presents time series of contributions from each source. Fig. 4 and Table 2 provide a comparison of seasonal contributions for each source and show the average source contributions for the whole period of sampling using the PMF model in Kalmiopsis site. The results of average source contributions for weekdays and weekend days are presented in Fig. 5.

The species contributing to the first source included OC2, OC3, OC4, EC1, EC2,  $\text{SO}_4^{2-}$ ,  $\text{NO}_3^-$ , K, and Mg. This profile was identified as wood/field burning. Because Kalmiopsis is surrounded by a large forest, wildfires and wood/field burning are common. In the case of rural communities, wood is a common domestic heating fuel. The peak seasonal mass contribution of wood/field burning source was the fall (53.6%,  $2.16 \mu\text{g m}^{-3}$ ). Table 2 shows that the average contribution during the fall were about three times higher than the contribution during the spring and contributes 38.4% ( $1.22 \mu\text{g m}^{-3}$ ) to the total  $\text{PM}_{2.5}$  mass concentration. Fig. 5 shows that weekday contributions ( $1.32 \mu\text{g m}^{-3}$ ) were somewhat higher than weekend contributions ( $1.00 \mu\text{g m}^{-3}$ ). In particular, wood/field-burning source showed high contribution during July 2002–September 2002 (Fig. 3).

On 13 July 2002, a wildfire began burning in the Biscuit Creek area (in the south Kalmiopsis roadless area) and continued to spread as far as the Rogue

Table 1  
Summary statistics for the PM<sub>2.5</sub> and species concentrations at Kalmiopsis site

	Kalmiopsis (ng m <sup>-3</sup> )						
	Arithmetic mean	Standard deviation	Geometric mean	Min.	Max.	No. of BDL <sup>a</sup> (%)	S/N ratio
PM <sub>2.5</sub> <sup>b</sup>	3.40	3.07	2.65	0.38	31.27	—	NA <sup>c</sup>
OC1	136.21	611.45	41.32	1.50	8419.30	385(77.8)	1.4
OC2	258.61	1238.01	121.18	9.10	25611.60	174(35.1)	8.3
OC3	671.44	1100.09	431.90	45.70	18198.90	30 (6.0)	90.3
OC4	313.15	733.10	209.00	37.00	14108.70	6 (1.2)	578.7
OP	95.44	180.89	61.32	2.90	3523.20	156(31.5)	8.0
EC1	135.71	345.75	77.92	2.90	6473.00	90(18.1)	20.4
EC2	49.14	57.97	35.91	2.80	984.30	161(32.5)	5.1
EC3	16.02	31.52	10.98	2.80	344.00	414(83.5)	0.6
SO <sub>4</sub> <sup>2-</sup>	486.81	373.04	323.18	7.70	2035.90	17( 3.4)	439.0
NO <sub>3</sub> <sup>-</sup>	146.62	150.50	93.85	0.20	2062.20	72(14.5)	35.4
Al	34.71	48.48	18.37	2.04	309.77	381(76.8)	3.2
As	0.31	0.63	0.21	0.03	8.32	239(48.2)	4.1
Br	1.23	1.90	0.90	0.05	39.77	0 (0.0)	NA
Ca	16.15	15.66	11.43	1.04	134.19	11 (2.2)	1531.2
Cl	111.37	169.96	35.99	0.28	1041.94	228(46.0)	132.2
Cr	0.54	0.63	0.20	0.02	2.23	425(85.7)	0.7
Cu	0.25	0.41	0.18	0.03	4.95	199(40.1)	7.4
Fe	13.43	21.03	6.15	0.35	193.87	0 (0.0)	NA
H	155.01	181.21	118.45	30.29	1998.62	0 (0.0)	NA
K	28.14	21.84	22.31	4.14	184.78	0 (0.0)	NA
Mg	26.59	16.29	22.07	5.96	75.93	424(85.5)	0.5
Mn	0.67	0.74	0.37	0.03	4.35	315(63.5)	2.1
Na	176.32	141.04	133.92	17.11	921.51	253(51.0)	5.4
Ni	0.21	0.43	0.15	0.03	5.99	301(60.7)	2.8
Pb	0.64	1.08	0.45	0.05	20.08	472(95.2)	93.8
Rb	0.14	0.11	0.12	0.01	0.81	269(54.2)	2.1
Se	0.09	0.06	0.08	0.02	0.34	213(42.9)	4.1
Si	57.38	78.53	31.87	1.42	683.09	55(11.1)	257.1
Sr	0.25	0.22	0.17	0.02	2.02	139(28.0)	11.3
Ti	2.47	2.86	1.28	0.04	20.59	198(39.9)	11.1
V	0.75	0.89	0.38	0.02	7.13	329(66.3)	1.8
Zn	1.73	2.23	1.15	0.10	31.04	5 (1.0)	3770.5

<sup>a</sup>Below detection limit.

<sup>b</sup>Unit  $\mu\text{g m}^{-3}$ .

<sup>c</sup>Not available (infinite S/N ratio caused by no BDL value).

River on 5 September 2002. More than 180,000 acres of the Kalmiopsis wilderness burned and the total area of fire was 500,000 acres (Harma and Morrison, 2003). The wood/field burning source contributions, TC (OC + EC; OC equals OC1 + OC2 + OC3 + OC4 + OP and EC equals EC1 + EC2 + EC3 – OP) concentration, K concentration, and SO<sub>4</sub><sup>2-</sup> concentration during the sampling period are compared and shown in Fig. 6 (gray box denotes the Biscuit wildfire periods). This figure shows that the high wood/field burning source contributions were in good agreement with high TC and K concentration during the Biscuit wildfire periods. The carbon/sulfate ratio during the nonsmoky

sample periods show an average value of  $2.6 \pm 2.0$ . During strong smoke events, the ratio can range 12–60 (VanCuren, 2003). In the case of Kalmiopsis data, the carbon/sulfate ratio was 11.6 during the Biscuit wildfire periods while the nonwildfire samples ratio was 4.1.

The PSCF plot for the wood/field burning source in Kalmiopsis site is presented in Fig. 7. This plot shows a major source area in the Siskiyou County and another in eastern Oregon. These results are in good agreement with the Biscuit wildfire site.

The species associated with the second source included SO<sub>4</sub><sup>2-</sup> and NO<sub>3</sub><sup>-</sup>, and these were classified as secondary sulfate and contributed 26.9% ( $0.85 \mu\text{g m}^{-3}$ )



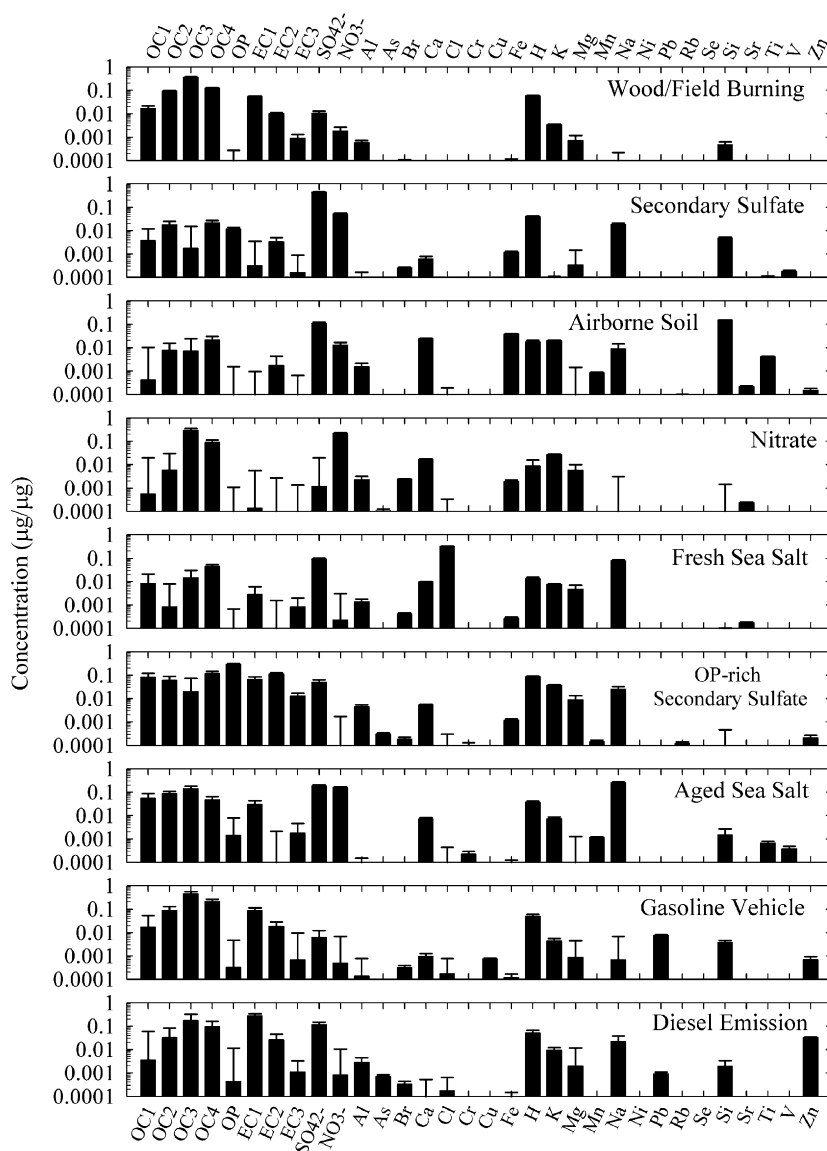


Fig. 2. Source profiles (prediction  $\pm$  standard deviation) of the resolved sources measured at the Kalmiopsis IMPROVE site.

to the total  $\text{PM}_{2.5}$  mass concentration. The average seasonal mass contributions show its peak contribution to be in the summer (Table 2). Although  $\text{NH}_4^+$  was not available to be included in the PMF modeling,  $\text{SO}_4^{2-}$  and  $\text{NH}_4^+$  would presumably exist as secondary sulfate such as  $(\text{NH}_4)_2\text{SO}_4$ . Fig. 5 shows there is no significant difference between the weekday versus the weekend concentrations. As shown in Fig. 7, the PSCF plot of secondary sulfate shows major potential source areas in western Washington, northwestern Oregon, and the near shore Pacific Ocean area where there are active shipping lanes.

Washington and Oregon have only one coal-fired power plant in each state. In the case of Washington, the Centralia Power Plant, with a production capacity of 1404 MW, is located in the southwest Washington. This plant emitted 83,600 t of  $\text{SO}_2$  in 2000. For Oregon, the Boardman power plant, with a production capacity of 600 MW, is situated in the north central Oregon. This plant emitted 14,374 t of  $\text{SO}_2$  in 2000 (Peele, 2003; US Environmental Protection Agency, 2005). The high PSCF values that lie in these areas could be related to  $\text{SO}_2$  emissions from coal-fired power plants. Moreover,

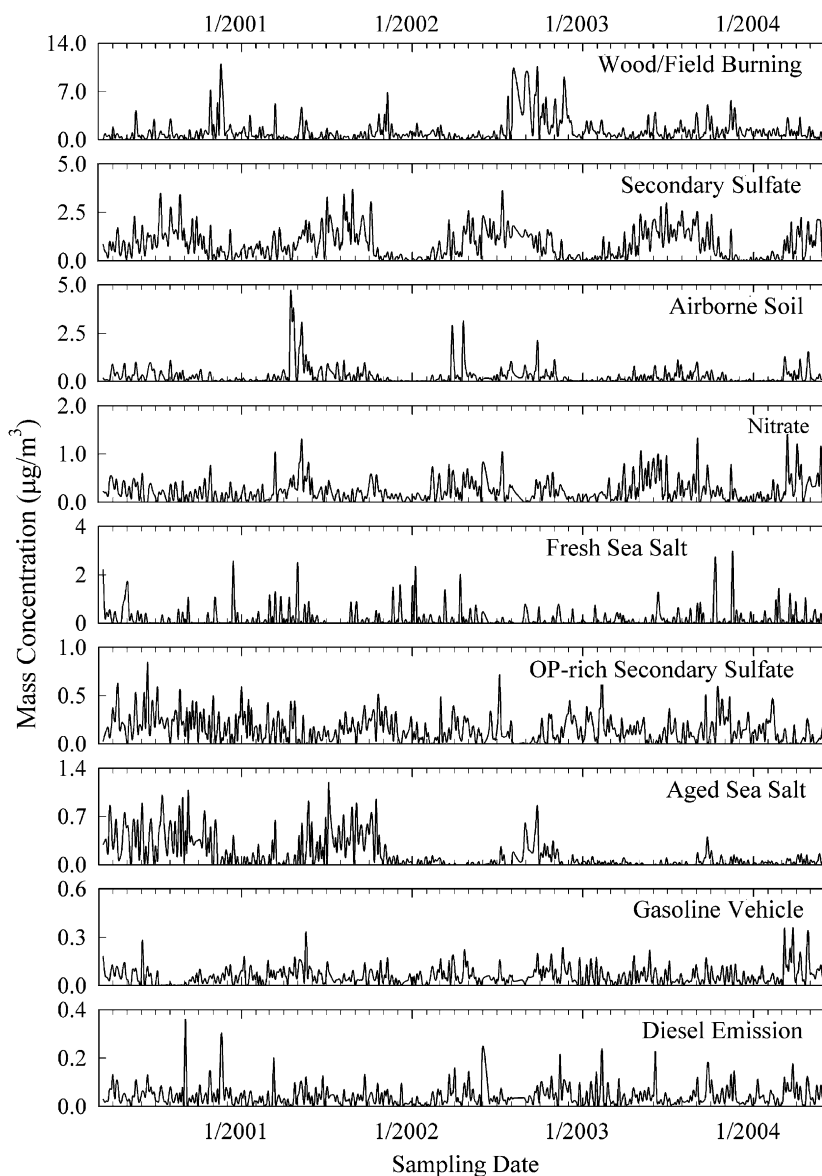


Fig. 3. Temporal variation of source contribution for the Kalmiopsis site constructed using the PMF model.

the pulp mills and petroleum refineries in these areas could contribute to the secondary sulfate concentrations. In the case of the Pacific Ocean, there are many ships burning high sulfur residual oil such that this area can contribute to the secondary sulfate source.

The third source was determined to be airborne soil. The major species contributing to this source included Si, Al, Ca, Fe, Ca, K, and Ti. The temporal variation of the source contribution plot shows very strong contributions in March and April 2001. The peak seasonal mass contribution of airborne soil

source was in the spring (14.8%,  $0.45 \mu\text{g m}^{-3}$ ). Fig. 5 shows that the average weekday contribution of airborne soil source ( $0.29 \mu\text{g m}^{-3}$ ) was somewhat higher than the weekend contribution ( $0.24 \mu\text{g m}^{-3}$ ). This source accounts for 8.6% ( $0.27 \mu\text{g m}^{-3}$ ) of the  $\text{PM}_{2.5}$  concentration. This seasonal pattern suggests the influence of intercontinental transport of Asian dust. Asian dust episodes have been observed at a number of sites in the western United States (VanCuren and Cahill, 2002; Liu et al., 2003a; Vancuren, 2003; Zhao and Hopke, 2004). The major intercontinental dust episodes are in March

and April. At higher altitudes, the impact of transported dust can also be observed at other times during the year (Liu et al., 2003a, b). Thus, the observed soil contributions during the remainder of the year are likely to be locally disturbed soils.

The fourth source profile includes a high concentration of  $\text{NO}_3^-$  and this source accounts for 7.6% ( $0.24 \mu\text{g m}^{-3}$ ) of the total  $\text{PM}_{2.5}$  mass concentration. In general, secondary nitrate is known to be seasonal with high contributions in winter because lower temperature and higher humidity help the formation of secondary nitrate particles (Seinfeld and Pandis, 1998). However, the seasonal average mass contributions of secondary nitrate show a peak in spring in this study. The reason for this behavior is not known.

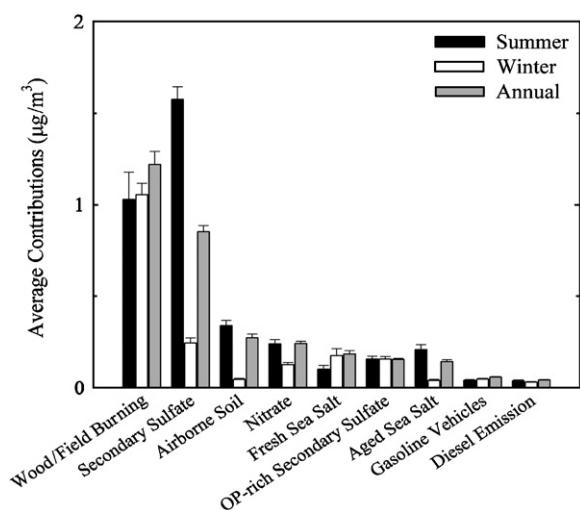


Fig. 4. Comparison of the seasonal contributions for each source in Kalmiopsis site.

Table 2

Average seasonal source contribution using the PMF model in Kalmiopsis IMPROVE site

	Winter		Spring		Summer		Fall		Avg.	
	( $\mu\text{g m}^{-3}$ )	%	( $\mu\text{g m}^{-3}$ )	%	( $\mu\text{g m}^{-3}$ )	%	( $\mu\text{g m}^{-3}$ )	%	( $\mu\text{g m}^{-3}$ )	%
Wood/field Burning	1.05	54.7	0.73	23.9	1.03	27.5	2.16	53.6	1.22	38.4
Secondary sulfate	0.25	12.7	0.89	29.1	1.58	42.2	0.74	18.4	0.85	26.9
Airborne soil	0.05	2.4	0.45	14.8	0.34	9.1	0.21	5.2	0.27	8.6
Nitrate	0.13	6.6	0.36	11.7	0.24	6.5	0.21	5.3	0.24	7.6
Fresh sea salt	0.18	9.1	0.26	8.3	0.10	2.7	0.18	4.6	0.19	5.8
OP + sulfate	0.16	8.2	0.13	4.3	0.16	4.2	0.18	4.5	0.16	4.9
Aged sea salt	0.04	2.1	0.12	3.7	0.21	5.6	0.22	5.6	0.14	4.5
Gasoline vehicle	0.05	2.5	0.08	2.7	0.04	1.1	0.06	1.5	0.06	1.9
Diesel emission	0.03	1.6	0.05	1.5	0.04	1.0	0.06	1.4	0.04	1.4
Sum	1.93	100.0	3.07	100.0	3.74	100.0	4.03	100.0	3.18	100.0

The species contributing to the fifth source include Cl, Na,  $\text{SO}_4^{2-}$ , Mg, K, and Ca. So, this source is assigned to be fresh sea salt and contributed 5.8% ( $0.19 \mu\text{g m}^{-3}$ ) to the total  $\text{PM}_{2.5}$  mass concentration. In the case of this source, the spring contribution was higher than other season contributions (spring  $0.26 \mu\text{g m}^{-3}$  > fall and winter  $0.18 \mu\text{g m}^{-3}$  > summer  $0.10 \mu\text{g m}^{-3}$ ). The fresh sea salt source showed no significant differences in the mean contributions between the weekdays versus weekends (Fig. 5).

The sixth source was classified as an OP-rich secondary sulfate with high abundances of OP and sulfate. A profile with high abundances of OP and sulfate has been reported in previous IMPROVE studies such as the Mammoth Cave National Park (Zhao and Hopke, 2006), Great Smoky Mountains National Park (Kim and Hopke, 2006), Bondville, IL (Kim et al., 2005a–c), and Washington, DC (Begum et al., 2005; Kim and Hopke, 2004a) studies. It accounts for 4.9% ( $0.16 \mu\text{g m}^{-3}$ ) of the  $\text{PM}_{2.5}$  mass concentration (Table 2). Yu et al. (2002) showed that an association between the water-soluble OC and OP formation in the thermal analysis of Hong Kong and China aerosols. It is suggested that the OP-rich secondary sulfate aerosols may be in part the result of heterogeneous acidic catalyzed reactions between the acidic sulfate and gaseous organic compounds that leads to additional secondary organic aerosol formation (Jang et al., 2003). The average mass contributions of OP-rich secondary sulfate show a peak in fall (Table 2). Similar to the secondary sulfate contributions, OP-rich secondary sulfate shows no difference between weekdays and weekend days (Fig. 5). In Fig. 7, the PSCF plot of OP-rich sulfate shows high



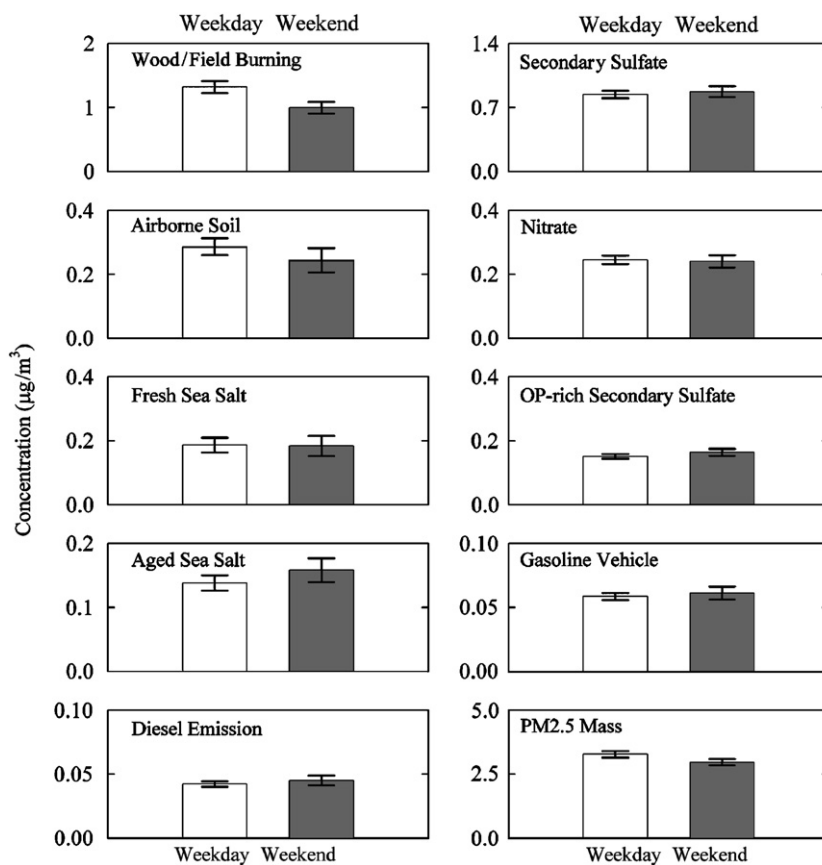


Fig. 5. The average source contributions for weekdays and weekend days in sampling site.

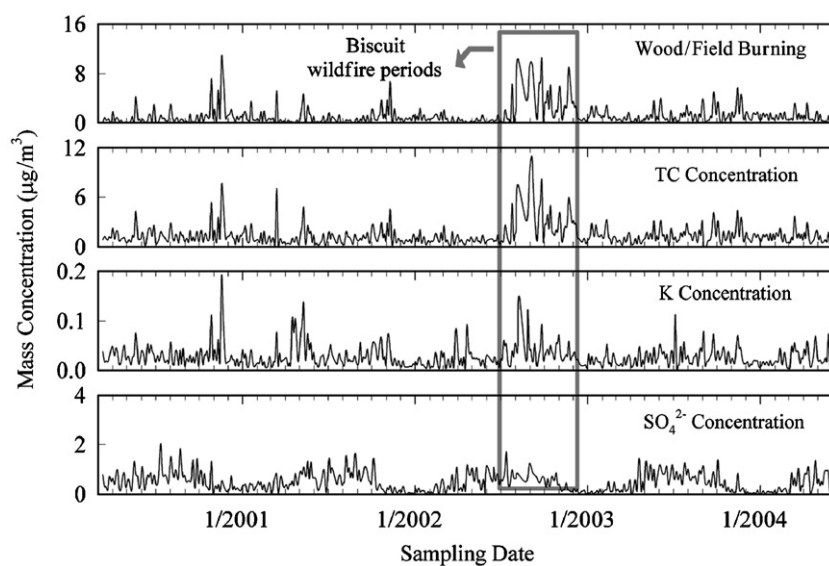


Fig. 6. Comparison between wood/field-burning source contributions and TC, K,  $\text{SO}_4^{2-}$  concentrations during the Biscuit wildfire periods.

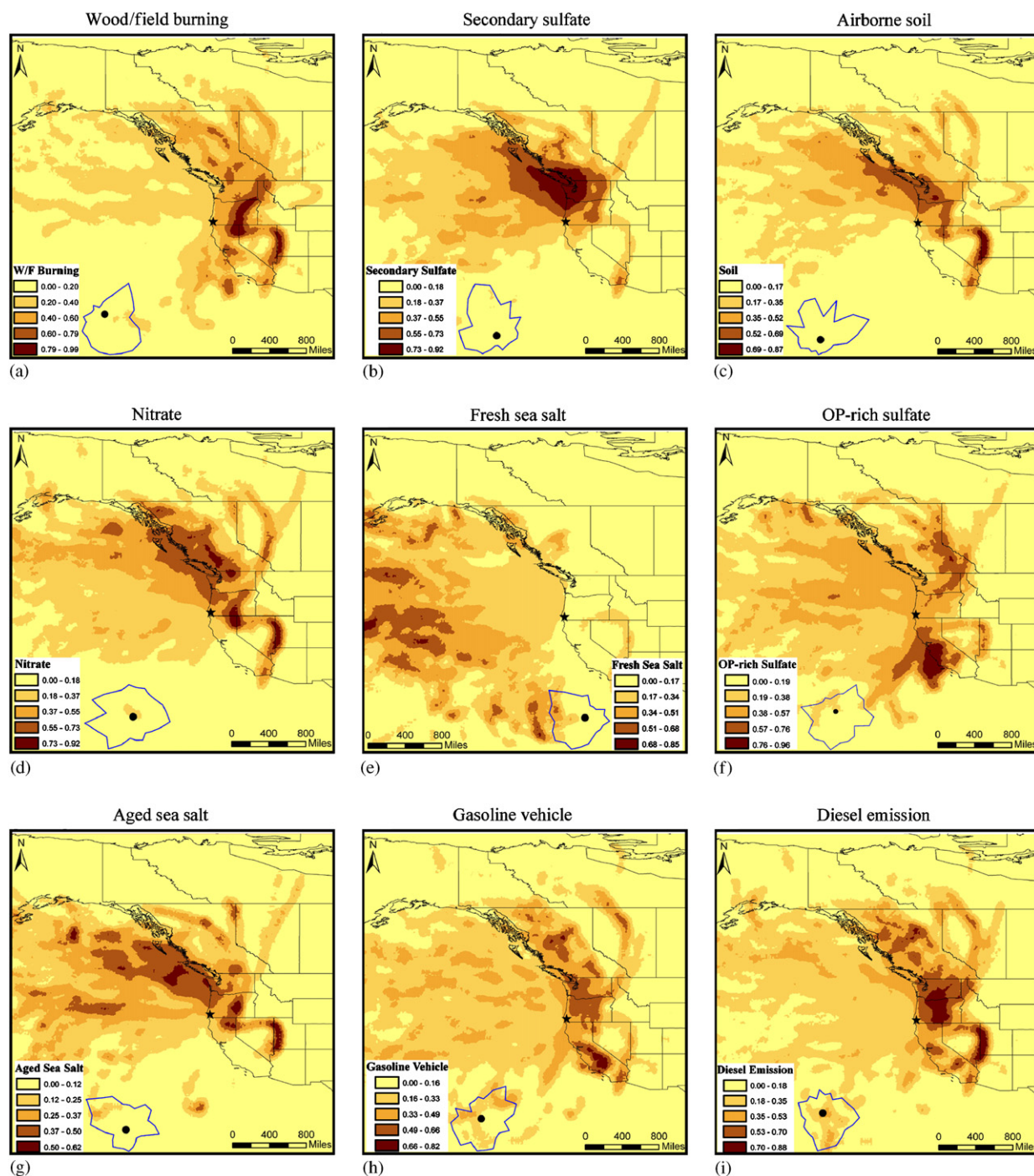


Fig. 7. Potential source contribution function plot for nine sources resolved by PMF in Kalmiopsis IMPROVE site (compare with conditional probability function plot below each PSCF plot).

potential areas in the forested regions of the western-central California, eastern Washington, and southern British Columbia in Canada. These areas are likely to be related to the OC emissions

from biogenic sources. The PSCF plot of OP-rich sulfate indicates regional influences of the biogenic as well as anthropogenic secondary aerosols. Further study is needed to understand the nature

of OP-rich sulfate source that has been found at most IMPROVE sites.

The major species contributing to the seventh source included Na,  $\text{SO}_4^{2-}$ ,  $\text{NO}_3^-$ , and Ca. These species suggest that this material is aged sea salt. The aged sea salt source peaked in the fall (fall  $0.22 \mu\text{g m}^{-3}$  > summer  $0.21 \mu\text{g m}^{-3}$  > spring  $0.12 \mu\text{g m}^{-3}$  > winter  $0.04 \mu\text{g m}^{-3}$ ). The aged sea salt source showed no significant difference between weekdays and weekend days (Fig. 5).

The eighth source profile was assigned to gasoline vehicle emissions. The OC3, OC4, and EC1 were major species contributing to the eighth source along with minor species such as Pb, Si, K, Ca, Mg, and Zn. This source was identified on the basis of high levels of OC, with a lower value of EC. The spring contributions ( $0.08 \mu\text{g m}^{-3}$ , 2.7%) were higher than for the other seasons (fall  $0.06 \mu\text{g m}^{-3}$ , winter  $0.05 \mu\text{g m}^{-3}$ , and summer  $0.04 \mu\text{g m}^{-3}$ ). Gasoline vehicle emissions showed no significant difference between the weekend and weekday contributions (Fig. 5). As shown in Fig. 7, the PSCF plot of gasoline vehicle emissions shows major potential source areas in central California, including Bakersfield, Fresno, and Sacramento. These areas are located between the Coastal Range and the Sierra Nevada Mountains. Interstate Highway 5 and California Highway 99 pass through these areas.

The species contributing to the ninth source profile are EC1, OC3, OC4,  $\text{SO}_4^{2-}$ , Na, K, Mg, Pb, Si, and Zn. The final source was identified as diesel emissions. The Si in the gasoline vehicle and diesel emissions profiles may be from associated road dust. The seasonal average mass contributions of diesel emission show a peak in fall ( $0.06 \mu\text{g m}^{-3}$ , 1.4%). Similar to the gasoline vehicle contributions, the diesel emissions showed no differences between weekdays and weekend days (Fig. 5).

Fig. 8 presents a comparison of the predicted  $\text{PM}_{2.5}$  contributions from all of the identified sources with measured  $\text{PM}_{2.5}$  concentrations. The PMF resolved sources effectively reproduced the measured values ( $R^2 = 0.97$ ) and account for most of the variation in the  $\text{PM}_{2.5}$  concentrations (slope = 0.898).

It was not possible to resolve a residual oil profile from these data and thus, there is no evidence of a direct impact of ship emissions on this site. The profiles for aged sea salt and secondary sulfate contain the highest concentrations of vanadium and nickel. Thus, the direct emissions from the residual

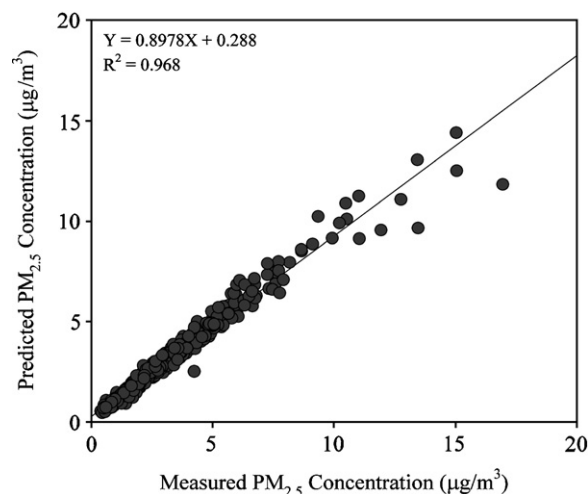


Fig. 8. Comparison of the predicted total  $\text{PM}_{2.5}$  mass concentrations from the PMF analysis with measured  $\text{PM}_{2.5}$  mass concentrations for the Kalmiosis IMPROVE site.

oil combustion in the ship engines has become fully admixed with the sources related to the sulfate and sea salt that has interacted with the sulfuric and nitric acid produced from the oxidation of the  $\text{SO}_2$  and  $\text{NO}_x$  emitted from the ships.

#### 4. Conclusion

This study identified the major sources of the ambient  $\text{PM}_{2.5}$  at the Kalmiosis IMPROVE site in southwestern Oregon. The sources were qualitatively identified and the source contributions were quantitatively estimated. The nine sources were identified as wood/field burning, secondary sulfate, airborne soil, secondary nitrate, fresh sea salt, OP-rich sulfate, aged sea salt, gasoline vehicle, and diesel emission source. Also, in order to identify potential source areas, a PSCF analysis was performed using the source contributions combined with backward trajectory data. The PSCF analysis identified the potential locations of the regional pollution sources of pollution. Wood/field-burning source is the largest  $\text{PM}_{2.5}$  source at the Kalmiosis site ( $1.22 \mu\text{g m}^{-3}$ , 38.4%) and the effect of a major wildfire (Biscuit fire) was identified. The PSCF analysis suggests the possible role for ship emissions of  $\text{SO}_2$  contributing to the secondary sulfate identified at the site. In this study, residual oil combustion source related to ship emission was not identified. However, impact of ship emissions is included in other sources. Thus, the direct particulate emissions from the ship that would include

vanadium and nickel had become admixed with the secondary sulfate and the sea salt that had reacted with the acidic byproducts of the ship emissions.

## Acknowledgments

This work was supported by California Air Resources Board under contract 04-326 and partly supported by the Korea Research Foundation Grant (KRF-2005-D00034-M01-2005-000-10022-0). The authors gratefully acknowledge the NOAA Air Resources Laboratory (ARL) for the provision of the HYSPLIT transport and dispersion model and/or READY website (<http://www.arl.noaa.gov/ready.html>) used in this publication.

## References

- Ashbaugh, L.L., Malm, W.C., Sadeh, W.D., 1985. A residence time probability analysis of sulfur concentrations at Grand Canyon National Park. *Atmospheric Environment* 19, 1263–1270.
- Begum, B.A., Hopke, P.K., Zhao, W., 2005. Source identification of fine particles in Washington, DC, by expanded factor analysis modeling. *Environmental Science and Technology* 39, 1129–1137.
- Calcabrin, A., Meschini, S., Marra, M., Falzano, L., Colone, M., Berardis, B.D., Paoletti, L., Arancia, G., Fiorentini, C., 2004. Fine environmental particulate engenders alterations in human lung epithelial A549 cells. *Environmental Research* 95, 82–91.
- Chan, Y.C., Simpson, R.W., Mctainsh, G.H., Vowles, P.D., Cohen, D.D., Bailey, G.M., 1999. Source apportionment of visibility degradation problems in Brisbane (Australia) using the multiple linear regression techniques. *Atmospheric Environment* 33, 3237–3250.
- Chow, J.C., Watson, J.G., Pritchett, L.C., Pierson, W.R., Fraizer, C.A., Purcell, R.G., 1993. The DRI thermal/optical reflectance carbon analysis system, description, evaluation and applications in US air quality studies. *Atmospheric Environment* 27A, 1185–1201.
- Chow, J.C., Watson, J.G., Crow, D., Lowenthal, D.H., 2001. Comparison of IMPROVE and NIOSH carbon measurements. *Aerosol Science and Technology* 34, 23–34.
- Chow, J.C., Watson, J.G., Chen, L.W.A., Miranda, G.P., Chang, M.C.O., Trimble, D., Fung, K.K., Zhang, H., Yu, J.Z., 2005. Refining temperature measures in thermal/optical carbon analysis. *Atmospheric Chemistry and Physics* 5, 2961–2972.
- Corbett, J.J., Fishbeck, P.S., 2000. Emissions from waterborne commerce vessels in United States Continental and Inland Waterways. *Environmental Science and Technology* 34, 3254–3260.
- Draxler, R.R., Rolph, G.D., 2003. HYSPLIT (hybrid single-particle Lagrangian integrated trajectory) model access via website (<<http://www.arl.noaa.gov/ready/hysplit4.html>>). NOAA Air Resources Laboratory, Silver Spring, MD.
- Gao, N., Cheng, M.D., Hopke, P.K., 1994. Receptor modeling of airborne ionic species collected in SCAQS. *Atmospheric Environment* 28, 1447–1470.
- Harma, K., Morrison, P.H., 2003. Assessment of the 2002 Biscuit fire complex in southwest Oregon and the landscape condition of the fire area. Pacific Biodiversity Institute.
- Harrison, R.M., Yin, J., 2000. Particulate matter in the atmosphere: which particle properties are important for its effects on health? *The Science of the Total Environment* 249, 85–101.
- Hsu, Y.K., Holsen, T.M., Hopke, P.K., 2003. Comparison of hybrid receptor models to locate PCB sources in Chicago. *Atmospheric Environment* 37, 545–562.
- Huffman, H.D., 1996. Comparison of the light absorption coefficient and carbon measures for remote aerosols: an independent analysis of data from the IMPROVE network. *Atmospheric Environment* 30 (1), 73–83.
- Hwang, I.J., Hopke, P.K., 2006. Comparison of source apportionments of fine particulate matter at two San Jose STN sites. *Journal of the Air and Waste Management Association* 56, 1287–1300.
- Jang, M., Lee, S., Kamens, R.M., 2003. Organic aerosol growth by acid-catalyzed heterogeneous reactions of octanal in a flow reactor. *Atmospheric Environment* 37, 2125–2138.
- Kim, E., Hopke, P.K., 2004a. Source apportionment of fine particles in Washington, DC, utilizing temperature-resolved carbon fractions. *Journal of the Air and Waste Management Association* 54, 773–785.
- Kim, E., Hopke, P.K., 2004b. Improving source identification of fine particles in a rural northeastern US area utilizing temperature resolved carbon fractions. *Journal of Geophysical Research* 109, D09204.
- Kim, E., Hopke, P.K., 2005. Improving source apportionment of fine particles in the eastern United States utilizing temperature-resolved carbon fractions. *Journal of the Air and Waste Management Association* 55, 1456–1463.
- Kim, E., Hopke, P.K., 2006. Characterization of fine particle sources in the Great Smoky Mountains area. *Science of the Total Environment* 368, 781–794.
- Kim, E., Hopke, P.K., Edgerton, E.S., 2003. Source identification of Atlanta aerosol by positive matrix factorization. *Journal of the Air and Waste Management Association* 53, 731–739.
- Kim, E., Hopke, P.K., Qin, Y., 2005a. Estimation of organic carbon blank values and error structures of the speciation trends network data for source apportionment. *Journal of the Air and Waste Management Association* 55, 1190–1199.
- Kim, E., Brown, S.G., Hafner, H.R., Hopke, P.K., 2005b. Characterization of non-methane volatile organic compounds sources in Houston during 2001 using positive matrix factorization. *Atmospheric Environment* 39, 5934–5946.
- Kim, E., Hopke, P.K., Kenski, D.M., Koeber, M., 2005c. Sources of fine particles in a rural midwestern US area. *Environmental Science and Technology* 39, 4953–4960.
- Lee, E., Chan, C.K., Paatero, P., 1999. Application of positive matrix factorization in source apportionment of particulate pollutants in Hong Kong. *Atmospheric Environment* 33, 3201–3212.
- Lee, J.H., Yoshida, Y., turpin, B.J., Hopke, P.K., Poirot, R.L., Lioy, P.J., Oxley, J.C., 2002. Identification of sources contributing to mid-Atlantic regional aerosol. *Journal of the Air and Waste Management Association* 52, 1186–1205.



- Liu, W., Hopke, P.K., VanCuren, R.A., 2003a. Origins of fine aerosol mass in the western United States using positive matrix factorization. *Journal of Geophysical Research* 108 (D23), 4716.
- Liu, W., Hopke, P.K., Han, Y.J., Yi, S.M., Holsen, T.M., Cybart, S., Kozlowski, K., Milligan, M., 2003b. Application of receptor modeling to atmospheric constituents at Potsdam and Stockton, NY. *Atmospheric Environment* 37, 4997–5007.
- Malm, W.C., Sisler, J.F., Huffman, D., Eldred, R.A., Cahill, T.A., 1994. Spatial and seasonal trends in particle concentration and optical extinction in the United States. *Journal of Geophysical Research* 99 (D1), 1347–1370.
- Paatero, P., 1997. Least squares formulation of robust non-negative factor analysis. *Chemometrics and Intelligent Laboratory Systems* 37, 23–35.
- Paatero, P., Hopke, P.K., 2003. Discarding or downweighting high-noise variables in factor analytic models. *Analytica Chimica Acta* 490, 277–289.
- Paatero, P., Hopke, P.K., Begum, B.A., Biswas, S.K., 2005. A graphical diagnostic method for assessing the rotation in factor analytical models of atmospheric pollution. *Atmospheric Environment* 39, 193–201.
- Paatero, P., Hopke, P.K., Song, X.H., Ramadan, Z., 2002. Understanding and controlling rotations in factor analytic models. *Chemometrics and Intelligent Laboratory Systems* 60, 253–264.
- Peele, C., 2003. Washington State mercury chemical action plan. Washington State Department of Health Publication No. 333-051.
- Polissar, A.V., Hopke, P.K., Paatero, P., Malm, W.C., Sisler, J.F., 1998. Atmospheric aerosol over Alaska 2. Elemental composition and sources. *Journal of Geophysical Research* 103 (D15), 19045–19057.
- Polissar, A.V., Hopke, P.K., Paatero, P., Kaufmann, Y.J., Hall, D.K., Bodhaine, B.A., Dutton, E.G., Harris, J.M., 1999. The aerosol at Barrow, Alaska: long-term trends and source locations. *Atmospheric Environment* 33, 2441–2458.
- Polissar, A.V., Hopke, P.K., Harris, J.M., 2001a. Source regions for atmospheric aerosol measured at Barrow, Alaska. *Environmental Science and Technology* 35, 4214–4226.
- Polissar, A.V., Hopke, P.K., Poirot, R.D., 2001b. Atmospheric aerosol over Vermont: chemical composition and sources. *Environmental Science and Technology* 35, 4604–4621.
- Qin, Y., Oduyemi, K., 2003. Atmospheric aerosol source identification and estimates of source contributions to air pollution in Dundee, UK. *Atmospheric Environment* 37, 1799–1809.
- Ramadan, Z., Song, X.H., Hopke, P.K., 2000. Identification of sources of Phoenix aerosol by positive matrix factorization. *Journal of the Air and Waste Management Association* 50, 1308–1320.
- Schwartz, J., Dockery, D.W., Neas, L.M., 1996. Is daily mortality associated specifically with fine particles? *Journal of the Air and Waste Management Association* 46, 927–939.
- Seinfeld, J.H., Pandis, S.N., 1998. *Atmospheric Chemistry and Physics, from Air Pollution to Climate change*. Wiley, New York.
- US Environmental Protection Agency, 1998. Guideline on speciated particulate monitoring. Research Triangle Park, NC.
- US Environmental Protection Agency, 2005. <<http://www.epa.gov/air/data>>.
- VanCuren, R.A., 2003. Asian aerosols in North America: extracting the chemical composition and mass concentration of the Asian continental aerosol plume from long-term aerosol records in the western United States. *Journal of Geophysical Research* 108 (D20), 4623.
- VanCuren, R.A., Cahill, T.A., 2002. Asian aerosols in North America: frequency and concentration of fine dust. *Journal of Geophysical Research* 107 (D24), 4804.
- Yu, J.Z., Xu, J.X., Yang, J., 2002. Charring characteristics of atmospheric organic particulate matter in thermal analysis. *Environmental Science and Technology* 36, 754–761.
- Zhao, W., Hopke, P.K., 2004. Source apportionment for ambient particles in the San Geronio wilderness. *Atmospheric Environment* 38, 5901–5910.
- Zhao, W., Hopke, P.K., 2006. Source identification for fine aerosols in Mammoth Cave National Park. *Atmospheric Research* 80 (4), 309–322.
- Zhou, L., Hopke, P.K., Liu, W., 2004. Comparison of two trajectory based models for locating particle sources for two rural New York sites. *Atmospheric Environment* 38, 1955–1963.